MAGNETIC MEASUREMENTS OF NICA BOOSTER DIPOLES

V. Borisov*, A.Bychkov, A.Donyagin, O. Golubitsky, H. Khodzhibagiyan ,
S. Kostromin, M.Omelyanenko, M.Shandov, A. Shemchuk , Laboratory of High Energy Physics,
Joint Institute for Nuclear Research, Dubna, Russia

Abstract

NICA is a new accelerator collider complex under construction at the Joint Institute for Nuclear Research in Dubna. NICA Booster magnetic system consists of 40 dipole and 48 quadrupole superconducting magnets. The magnetic field parameters of each magnet must be measured. At the moment 13 series dipole magnets are assembled and have successfully passed all the tests. Booster dipole magnets are 2.14 m-long, 128 /65 mm (h/v) aperture magnets with design similar to Nuclotron dipole magnet but with curved (14.1 m radius) yoke. They are designed to create magnetic fields up to 1.8 T. magnetic field parameters will be measured at "warm" (300 K) and "cold" (4.5 K) conditions. This paper describes magnetic measurements methods and developing of magnetic measurements system. The obtained results of magnetic measurements of 13 magnets are summarized here.

INTRODUCTION

The NICA accelerator complex [1], [2] will include 600 MeV/u Booster synchrotron as a part of the heavy ion injection chain of the NICA Collider. The Booster [3] of the NICA accelerator complex is a superconducting synchrotron which will be placed inside the yoke of the former Synchrophasotron. NICA Booster magnetic system consists of 40 dipole and 48 quadrupole superconducting magnets. The technical complex [4] for assembly and testing of SC magnets for the NICA and FAIR project at the Laboratory of High Energy Physics (LHEP) is operating in assembling and series testing mode. At the moment, 13 dipole magnets have been manufactured and fully tested. The designs of the magnets for the NICA booster are given in [5], [6]. The main characteristics of the dipole magnet for the NICA booster are presented in the Table 1.

Table 1: Main characteristics of the NICA Booster Magnets

Parameter	Unit	Value
Number of magnets		40
Magnetic field (inj./max.)	T	0.11 /1.8
Effective magnetic length	m	2.2
Beam pipe aperture (h/v)	mm	128 /65
Bending angle	deg	9
Radius of curvature	m	14.01
Operating current	kA	9.68
Field error at R= 30 mm		$\leq 6 \cdot 10^{-4}$

The boosters operating cycle consists of stages of linear field ramping up and down with a ramp rate of 1.2 T/s and two stages of a constant field: the stage of injection magnetic field of 0.11 T and the stage of electron cooling of 0.56 T. According to the specification, the following parameters of dipole magnets of the booster have to be measured:

- Relative standard deviation of effective lengths

$$L_{eff} = \frac{\int_{-\infty}^{\infty} B_y ds}{B_y(0)} \qquad \delta L_{eff} = \frac{\Delta L_{eff}}{< L_{eff} >} \leq 5 \cdot 10^{-4}$$

- Magnetic field direction (dipole angle), angle between the magnetic and mechanical median plane

$$\alpha_1 = -arctg(\frac{A_1^*}{B_1^*}) \qquad \sigma(\alpha_1) \leq 0.1 \ mrad$$

* - integrated harmonics

- Relative integrated harmonics up to the 5th

b_2^* , a_2^* , a_3^*	$\leq 5 \cdot 10^{-4}$
b_3^*	$\leq 10^{-3}$
b_3^* at injection	$\leq 10^{-4}$
b_n^* , a_n^* , $n>3$	$\leq 10^{-4}$

MAGNETIC MEASUREMENTS

Magnetic measurements have been performed using the rotating harmonic coils probes. The step-by-step method of measurement with fast-ramped magnetic field with ramp rate 1.2 T/s was used. Detailed description of the magnetic measurement system and methods was done in papers [7], [8]. The magnetic measuring system
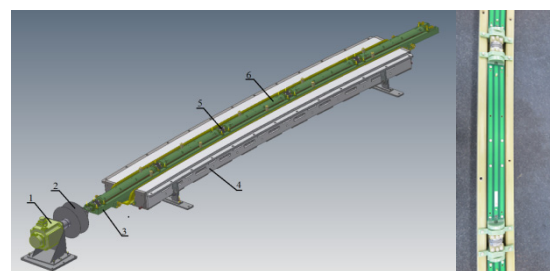

Figure 1: Layout of bottom part of magnets yoke with installed MMS: 1. Servomotor, 2. Bobbin for the cable, 3. Base frame, 4. Bottom part of yoke, 5. Flexible coupling, 6. Measuring section.

(MMS) (see Fig. 1) consists of five identical sections connected among themselves by bellows couplings. Each

section has inside three measuring coils made as a single multilayered printed-circuit board. Pins on the bottom pole of a magnet yoke fix the base frame. Coils consist of 400 turns created from 20 layers, each of which contains 20 turns. Both types of magnetic measurements, "warm" and "cold", have been performed using same MMS. Temperature of MMS (in range 100-70 K) was controlled by TVO sensors. Corrections of harmonic coils dimensions were applied in harmonics calculations.

MAGNETIC MEASUREMENTS RESULTS

At the moment 13 dipole magnets, (are one third of all,-) are assembled and have passed all the tests, including "warm" and "cold" magnetic measurements. The results are presented on figures 5-10.
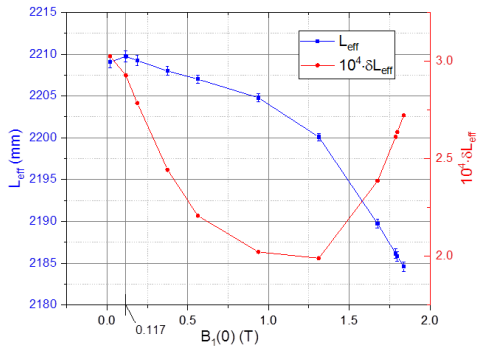

Figure 2: Mean value and relative standard deviation of effective lengths vs. the magnetic field induction in the center. 0.117 T is injection field.

Effective Length

To calculate the relative variation of dipoles effective lengths, the value approximately equal to the effective length was calculated:

$$L_{eff} = \frac{1}{B_1(0)} \left[\sum_{i=1}^{5} B_{1,i} \cdot s_i \right]$$

i - section number, $B_{1,i}$ - main field harmonic measured by i section, s_i – part of integration path going thru i
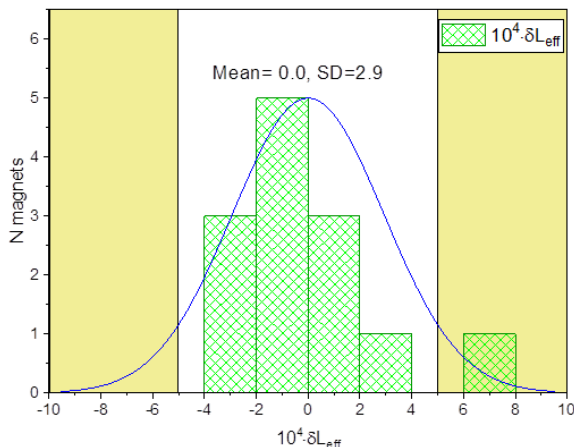

Figure 3: Distribution of effective lengths relative variations for maximum RSD.

section, $B_1(0) = B_{1,3}$. Sections 1 and 5 cover edge field regions, $s_1 = s_5 = l_{coil}$. Sections 2, 3 and 4 cover plateau field region with path s_{1-5} between coils 1 and 5, this path is divided on three equal parts $s_{2(3,4)}$. Mean value and relative standard deviation (RSD) of effective lengths are displayed in Fig. 2 as a function of the magnet excitation. RSD of all magnets is in accordance with requirements of specifications. Fig. 3 shows the distribution of effective lengths relative variations for maximum RSD. We can see that for only one magnet the effective length is out from specification.

Dipole Angle

To create a reference point for field direction measurements we use the reference magnetic field created by the additional pointlike windings so, that it is parallel to the surfaces of the poles. We measure phases of the main harmonics of the reference field as initial angles of coils rotation. Average reproducibility (random error) of initial angles is better than 0.1 mrad. High accuracy and
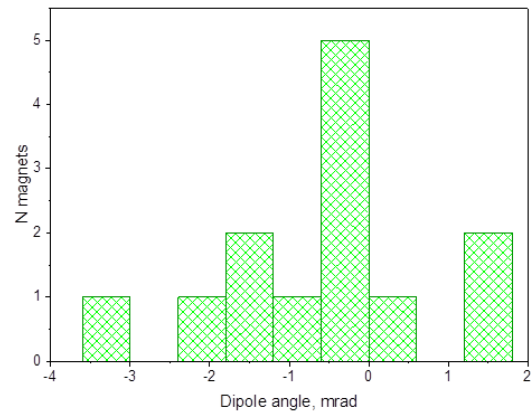

Figure 4: Distribution of dipole angle.

high resolution servomotor is used to reproduce initial angles with required accuracy. Distribution of the dipole angle for measured magnets is displayed in Fig.4.
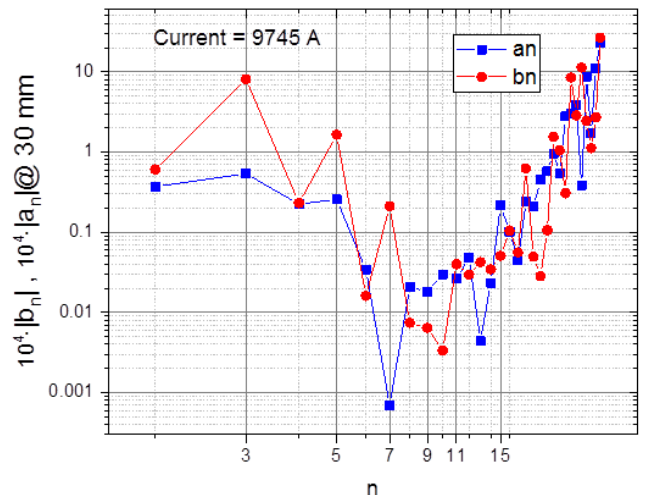

Figure 5: Harmonics vs harmonic number.

Relative Integrated Harmonics

We use analog compensation for harmonics measurement. The compensation ratio for various sections are in range 1600-21000. Such high values of compensation ratio are possible due to the very precise geometry of the coils made as PCBs. Typical dependence of all measured harmonics on harmonics number is shown at Fig. 5. We can see that noise floor is 0.01 unit. At the reference radius 30 mm, what is larger then external coil
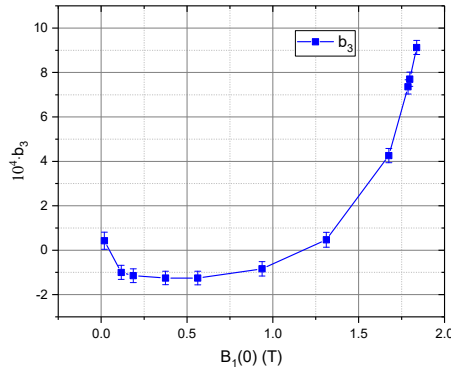

Figure 6: b_3 harmonic vs. the magnetic field induction in the center.

radius R_{coil}= 22.3 mm, we can measure harmonics up to n=7 (as required by specification). The most critical harmonic is b_3. Dependence of mean value of b_3 harmonic with standard deviations is shown at Fig. 6. On fig.7 we can see that for some magnets the distribution of b3 harmonic at injection field level exceeds specified
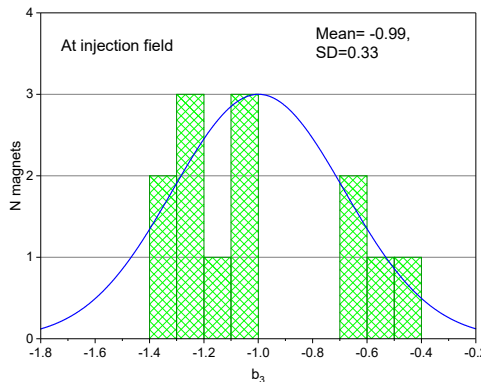

Figure 7: Distribution of b_3 harmonic at injection field.

tolerance. At the maximum field level, the b3 of all the magnets corresponds to the specification. The level of a_2, a_3 and b_2 harmonics (see Fig.8) meet the specification.

CONCLUSION

One thirds of the dipole magnets for the NICA booster synchrotron was successfully passed cryogenic test and can be installed in the tunnel of the accelerator. Magnetic measurements have showed good correspondence of the magnetic field parameters of magnets to the requirements of the specification.
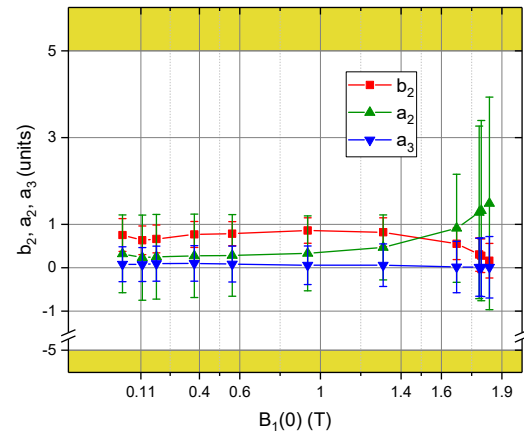

Figure 8: a_2, a_3 and b_2 harmonics vs the magnetic field induction in the center.

REFERENCES

[1] Nuclotron - based ion collider facility. Available: http://nica.jinr.ru/

[2] G. Trubnikov et al., "NICA project at JINR", Proceedings of IPAC2013, Shanghai, 2013, pp. 1343 – 1345.

[3] A. Tuzikov *et al.*, "Booster Synchrotron at NICA Accelerator Complex", in *Proc. 25th Russian Particle Accelerator Conf. (RuPAC'16)*, St. Petersburg, Russia, Nov. 2016, paper FRCAMH05, pp. 160-162, doi:10.18429/JACoW-RuPAC2016-FRCAMH05, ISBN:978-3-95450-181-6.

[4] H.G. Khodzhibagiyan *et al.*, "The Progress on Manufacturing and Testing of the SC Magnets for the NICA Booster Synchrotron", in *Proc. 25th Russian Particle Accelerator Conf. (RuPAC'16)*, St. Petersburg, Russia, Nov. 2016, paper THCDMH03, pp. 144-146, doi:10.18429/JACoW-RuPAC2016-THCDMH03, ISBN:978-3-95450-181-6.

[5] H. Khodzhibagiyan *et al.*, "Superconducting Magnets for the NICA Accelerator Collider Project", *IEEE Trans. Appl. Supercond.*, vol.26, N3, June 2016.

[6] H. Khodzhibagiyan *et al.*, "Superconducting Magnets for the NICA Accelerator-Collider Complex", *IEEE Trans. Appl. Supercond.*, vol.24, N3, pp. 4001304, June 2014.

[7] V. Borisov *et al.*, "Magnetic measurement system for the NICA booster magnets," in Proceedings of the 5th International Particle Accelerator Conference IPAC 2014, Dresden, Germany, June 15–20, 2014, p. 2696, paper WEPRI088.

[8] S. A. Kostromin *et al.*, "Measurement of the Magnetic-Field Parameters of the NICA Booster Dipole Magnet", *Physics of Particles and Nuclei Letters*, 2016, Vol. 13, No. 7, pp. 855–861.